ISSN 1674-1056
http://cpb.iphy.ac.cn
http://iopscience.iop.org/cpb
中国物理 B
Chinese Physics
中国物理 Chinese Physics B

Experimental and numerical study on energy dissipation in freely cooling granular gases under microgravity

Wen-Guang Wang(王文广), Mei-Ying Hou(厚美瑛), Ke Chen(陈科), Pei-Dong Yu(虞培东), Matthias Sperl

Citation: Chin. Phys. B . 2018, 27(8): 084501. **doi:** 10.1088/1674-1056/27/8/084501

Journal homepage: http://cpb.iphy.ac.cn; http://iopscience.iop.org/cpb

What follows is a list of articles you may be interested in

Ultrasound wave propagation in glass-bead packing under isotropic compression and uniaxial shear

Zhi-Gang Zhou(周志刚), Yi-Min Jiang(蒋亦民), Mei-Ying Hou(厚美瑛)

Chin. Phys. B . 2017, 26(8): 084502. **doi:** 10.1088/1674-1056/26/8/084502

X-ray tomography study on the structure of the granular random loose packing

Yi Xing(邢义), Yu-Peng Qiu(邱宇鹏), Zhi Wang(王智), Jia-Chao Ye(叶佳超), Xiang-Ting Li(李向亭)

Chin. Phys. B . 2017, 26(8): 084503. **doi:** 10.1088/1674-1056/26/8/084503

DEM simulation of granular segregation in two-compartment system under zero gravity

Wenguang Wang(王文广), Zhigang Zhou(周志刚), Jin Zong(宗谨), Meiying Hou(厚美瑛)

Chin. Phys. B . 2017, 26(4): 044501. **doi:** 10.1088/1674-1056/26/4/044501

Granular packing as model glass formers

Yujie Wang(王宇杰)

Chin. Phys. B . 2017, 26(1): 014503. **doi:** 10.1088/1674-1056/26/1/014503

The anisotropy of free path in a vibro-fluidized granular gas

Yifeng Mei(梅一枫), Yanpei Chen(陈延佩), Wei Wang(王维), Meiying Hou(厚美瑛)

Chin. Phys. B . 2016, 25(8): 084501. **doi:** 10.1088/1674-1056/25/8/084501

Experimental and numerical study on energy dissipation in freely cooling granular gases under microgravity*

Wen-Guang Wang(王文广)[1,2], Mei-Ying Hou(厚美瑛)[1,2,†], Ke Chen(陈科)[1,2], Pei-Dong Yu(虞培东)[3], and Matthias Sperl[3]

[1] *Key Laboratory of Soft Matter Physics, Beijing National Laboratory for Condensed Matter Physics, Institute of Physics, Chinese Academy of Sciences, Beijing* 100190, *China*

[2] *School of Physical Sciences, University of Chinese Academy of Sciences, Beijing* 100049, *China*

[3] *Institut für Materialphysik im Weltraum, Deutsches Zentrum für Luft-und Raumfahrt, Köln* 51170, *Germany*

(Received 8 April 2018; revised manuscript received 17 April 2018; published online 10 July 2018)

Energy dissipation is one of the most important properties of granular gas, which makes its behavior different from that of molecular gas. In this work we report our investigations on the freely-cooling evolution of granular gas under microgravity in a drop tower experiment, and also conduct the molecular dynamics (MD) simulation for comparison. While our experimental and simulation results support Haff's law that the kinetic energy dissipates with time t as $E(t) \sim (1+t/\tau)^{-2}$, we modify τ by taking into account the friction dissipation during collisions, and study the effects of number density and particle size on the collision frequency. From the standard deviation of the measured velocity distributions we also verify the energy dissipation law, which is in agreement with Haff's kinetic energy dissipation.

Keywords: granular gas, freely cooling, microgravity

PACS: 45.70.–n, 45.70.Mg **DOI:** 10.1088/1674-1056/27/8/084501

1. Introduction

Granular gas is a dilute ensemble of grains interacting by dissipative collisions. This dissipative nature of particle interactions determines its ensemble properties, and distinguishes it from molecular gas. The most prominent feature is granular cooling so that the system loses kinetic energy permanently, with no external energy input. From a homogeneous excited-state, the system enters into an initial period of homogeneous energy loss, and later grains can spontaneously cluster.[1–17] Theoretical modeling,[18–29] and simulation investigations[20–22,24,28,30–39] are based on simplifications and assumptions of grain properties. Quantitative experiments are very much needed for better understanding of fundamental features of such ensembles.[40–43] In this work we report our investigations on the freely-cooling evolution of granular gas under microgravity in a drop tower experiment, and conduct the molecular dynamics (MD) simulation for comparison.

In order to investigate the energy loss due to grain-grain collisions in steady excitation and during free cooling, experiments need to counterbalance the gravitational force to float the particles.[14,40] In 2008, Maaß *et al.* used magnetic forces to make the granular particles float in a container.[40] In their experiment, diamagnetic particles were chosen. The total energy of a particle in a magnetic field B is $U = -\chi V B^2/2\mu_0 + mgz$,[44] where U is the potential energy of the particle, χ is the magnetic susceptibility, V is the volume of the particle, μ_0 is vacuum permeability, m is the mass of particle, g is the gravity, and z is the position of particle in the z direction. Since $\boldsymbol{F} = -\nabla U$ and the force balance requires $\boldsymbol{F} = 0$, $-\nabla U = -mg\boldsymbol{e}_z + \chi V \boldsymbol{B}\nabla\boldsymbol{B}/\mu_0 = 0$ and $\boldsymbol{B}\nabla\boldsymbol{B} = \mu_0\rho g/\chi$, where $\rho = m/V$ is the density of particle. Since $\nabla^2 U = -\chi V \nabla^2 \boldsymbol{B}^2/2\mu_0$ and $\nabla^2\boldsymbol{B}^2 > 0$, for diamagnetic particles $\chi < 0$, $\nabla^2 U > 0$, therefore the diamagnetic particles can float stably in such an external magnetic field. Maaß *et al.* used this method to make the particles float. They have successfully observed two stages. At early time, the evolution of the kinetic energy dissipation of granular gas follows Haff's law. At a later time, the granular gas clusters and behaves like a single particle motion, which depends on the size of the container.

Tatsumi *et al.* reported in 2009 the first microgravity experimental investigations on a freely cooling granular gas system. Their microgravity experiment was performed during parabolic flight. They studied the kinetics of both freely cooling and steadily driven granular gas system in quasi-two-dimensional cells under micro-gravity.[41] Due to the g-jitter of the parabolic flights, Tatsumi *et al.* could observe only within one second of the cooling process. Their granular temperature decays as $T_g = T_0(1+t/\tau)^{-2}$, which is consistent with Haff's law that $E(t) \sim (1+t)^{-2}$.

Very recently Kirsten Harth *et al.* studied free cooling of a granular gas of rod-like particles in microgravity. For rod-like particles they found that the law of $E(t) \sim t^{-2}$ is still robust.[43] A slight predominance of translational motions, as well as a preferred rod alignment in the flight direction were

*Project supported by the National Natural Science Foundation of China (Grant Nos. U1738120 and 11474326).

†Corresponding author. E-mail: mayhou@iphy.ac.cn

© 2018 Chinese Physical Society and IOP Publishing Ltd

also found.

These previous studies mainly concerned the form of kinetic energy dissipation with time. In this paper, we conduct a micro-gravity experiment in a Bremen Drop Tower and compare the results with simulations to verify the validation of more detailed factors (such as restitution coefficient, number density, particles size) affecting Haff's law. We take into consideration the collision friction to modify the model for the characteristic decay time τ. Experimental and simulation results show that the average speed of all particles in granular gas decays with time t as $v \sim (1+t/\tau)^{-1}$ and the kinetic energy decays with time t as $E(t) \sim (1+t/\tau)^{-2}$ as predicted in Haff's law. In our 5 second cooling observation time we, however, do not see the clustering mode as reported in Maaß's research.

2. Haff's freely cooling model

Haff's theory about freely cooling granular is based on the classical thermodynamics.[18,19] There are several assumptions to simplify the analysis of the freely cooling process of dilute granular gas. Firstly, the restitution coefficient is constant for each collision among particles. Secondly, the granular gas system must be homogeneous, so the mean free path is meaningful in the analysis and can be used to calculate the collision frequency. Thirdly, only collisions among particles contribute to the energy dissipation in the theory, while the part due to friction is not taken into account. Fourthly, the size of particles is relatively small compared with the mean free path.

The mean free path of particles in dilute and homogeneous granular gas is $\lambda = 1/(n\sigma)$, where n is the number density and $\sigma = \pi(2R)^2$ is the cross section of particle respectively. Here R is the particle radius. The kinetic energy E of one-unit volume of granular gas is proportional to $nm\bar{v}^2/2$, namely $E \propto nm\bar{v}^2/2$, where $\bar{v}$ is the average speed of particles. When a particle collides with another one, the average kinetic energy loss of a collision is proportional to $\left(1-e^2\right)m\bar{v}^2/2$. The collision frequency of a single particle, is $\bar{v}/\lambda$. The collision frequency of the whole system will be $n\bar{v}/\lambda$; however, a single collision between two particles is counted twice in a whole system, the actual collision frequency of the system is $n\bar{v}/2\lambda$. The total kinetic energy loss per unit time of one-unit volume of granular gas is

$$\Delta E = -\frac{\left(1-e^2\right)nm\bar{v}^3}{4\lambda}. \tag{1}$$

The change of kinetic energy per unit time equals the loss of the energy per unit time due to collisions between particles,

$$\frac{\mathrm{d}}{\mathrm{d}t}\left(\frac{1}{2}nm\bar{v}^2\right) = -\left(1-e^2\right)\frac{nm\bar{v}^3}{4\lambda}. \tag{2}$$

By solving Eq. (2), the solution is

$$\bar{v}(t) = \frac{\bar{v}_0}{1+t/\tau}, \tag{3}$$

$$\tau = \frac{4}{\left(1-e^2\right)\bar{v}_0 n\sigma}, \tag{4}$$

where $\bar{v}_0$ is the initial average speed of the granular particles. We notice that equation (4) is different from that used in Maaß's research[40] by a factor of 2. Our simulation results support Eq. (4).

The kinetic energy E is proportional to $\bar{v}^2$, the evolution of kinetic energy, thus, is

$$E = \frac{E_0}{(1+t/\tau)^2}. \tag{5}$$

After a duration of τ since the granular gas begins to cool freely, the average velocity of the system will drop by half as given in Eq. (3). This parameter has also been used in Brilliantov and Pöschel's paper,[29,41] that is,

$$\tau^{-1} = 2\sqrt{\frac{T_0}{\pi}}\left(1-e^2\right)\frac{1-(7/16)\,\phi}{(1-\phi)^2}\frac{\phi}{d}, \tag{6}$$

where T_0 is the initial granular temperature, d is the diameter of particle, and ϕ is the volume friction. In order to compare with their work, we also study the dependence of characteristic decay time τ on material parameters (the restitution coefficient e and the particle size R), and also the initial velocity of the system, $\bar{v}_0$. The τ dependence shows the complex property of granular matter – the historical dependency.

Most of the previous research has mainly been concerned with the form of Eq. (3), and the exact expression of τ is not yet unique. Hence, we pay more attention to the characteristic decay time τ here, and our numerical results support the form of Eq. (4).

3. Experiment

To study the granular gas cooling behavior on the ground, gravity has to be counteracted by an external force, like buoyancy in liquid, an electric or magnetic field force. For example, Maaß *et al.* used the magnetic gradient to make the diamagnetic particle float.[40] Soichi Tatsumi *et al.* were the first to attempt microgravity experiment studying the freely cooling granular gas behavior in parabolic flights.[41] However, due to the g-jitter during the flights, their cooling observations were no longer than 1.6 s. In the present work, we achieve microgravity in a Bremen Drop Tower. The Bremen Drop Tower, with a height of 146 meters, provides up to 10^{-6}-g microgravity condition with a duration as long as 9.3 s.

In our experiments, the catapult operation mode with a weightless duration of 9.3 s was adopted. By this means, a drop capsule [see Figs. 1(a) and 1(b) was thrown from the

bottom of the tower to the top and back into a buffer container filled with foam pellets. Before the freely cooling phenomenon is observed, the particles had to move at a certain initial velocity. In the initial 3 s or 4 s, the granular gases were driven by two pistons which were controlled by two linear motors separately [Fig. 1(c). Then the motor was powered off, the process of freely cooling started. A high-speed camera was used to process and analyze the particle trajectories.

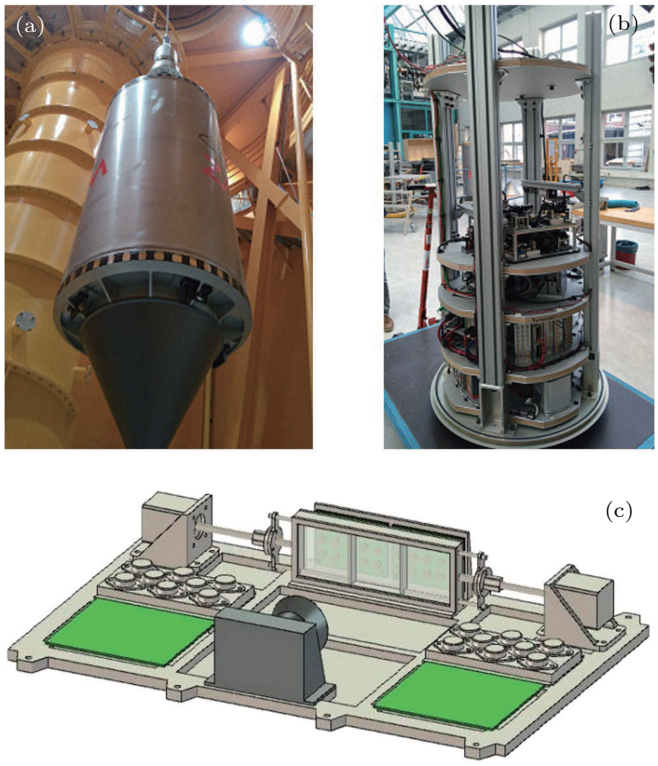


Fig. 1. (color online) (a) Experiment setup carrying drop capsule; (b) experiment platform composed of the power system and the setup; (c) sketch of the experimental setup.



Fig. 2. (color online) Sample cell where two pistons are marked by red dash lines.

The size of the sample cell is 150 mm×50 mm×10 mm. Three sub cells are separated by two pistons as is shown in Fig. 2. The numbers of particles in each subcell from left to right in Fig. 2 are 171, 286, and 64, respectively. The diameters of particles in each subcell from left to right are 2.5 mm, 2 mm, and 2.5 mm, respectively. Particle motions are initiated by the two pistons, whose central positions, vibration frequencies, and amplitudes are controlled. The pistons are stopped after 3 s to 4 s for the fast camera to take images of grain motion during cooling. The image data in the middle and the right subcell are processed and analyzed. Two drop experiments are conducted. The key parameters in each experiment are shown in Table 1.

Table 1. Key parameters in each group of experiments.

Index	Particle number	Particle size/mm	Cell length/mm	Number density/cm^{-3}	Volume fraction
1	286	2	67	8.5	0.036
2	286	2	68	8.4	0.035
3	64	2.5	40	3.2	0.026
4	64	2.5	35	3.7	0.030

4. Experimental results

The experimental images are captured by a high-speed camera of 500 fps. Each frame of the image is of 512 × 512 pixels. The resolution of experimental images is about 0.3 mm/pixel, therefore the particle sizes with diameters 2 mm and 2.5 mm are about 6–7 pixels and 8–9 pixels, respectively. However, since we have only one camera, we can observe only a two-dimensional projection of the particle three-dimensional motion. Some trajectories of two overlapped particles may not be identified. Over exposure in one of the cell corners also hinders tracing particles in that area. Despite of all these, we can trace more than 95 percent of the total particles.

Figure 3(a) shows the trajectories of all the traceable particles in the freely cooling processes. Not all the particles can be traced at all times. The average end speeds of particles in these four sets of experiments are about 4 mm/s–5 mm/s. The average speed decreases by an order of magnitude in 4 s–5 s. Figure 3(b) shows that many particles move in a local area before they cool down.

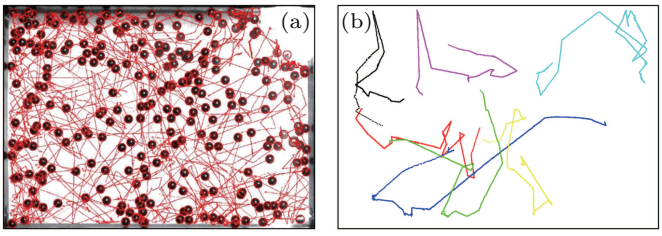


Fig. 3. (color online) (a) Traces of all particles in the freely cooling process; (b) Demo of few traces of particles.

The speed of each particle v_i is calculated from $v_i = \sqrt{v_{ix}^2 + v_{iy}^2}$, where v_{ix} is the i-th particle velocity along the excitation direction, and v_{iy} is the velocity of the particle along the perpendicular y direction. The $\bar{v}$ denotes the average velocity of all particles. Here we set the mass of a particle $m = 1$, so the average kinetic energy is $\bar{E} = \langle v_i^2 \rangle$. In Fig. 4 we fit the average speed and the average kinetic energy of particles by Haff's law. It is seen that Haff's equation fits well, although it does not take into consideration the inelastic collisions with the rigid

walls nor frictions in the particle–particle collisions. The values of the two fitting parameters in Haff's law $\bar{v}_0/(1+t/\tau)$, i.e., $\bar{v}_0$ (the initial average speed) and τ (the decay time), in the four sets of experiments are given in Table 2.

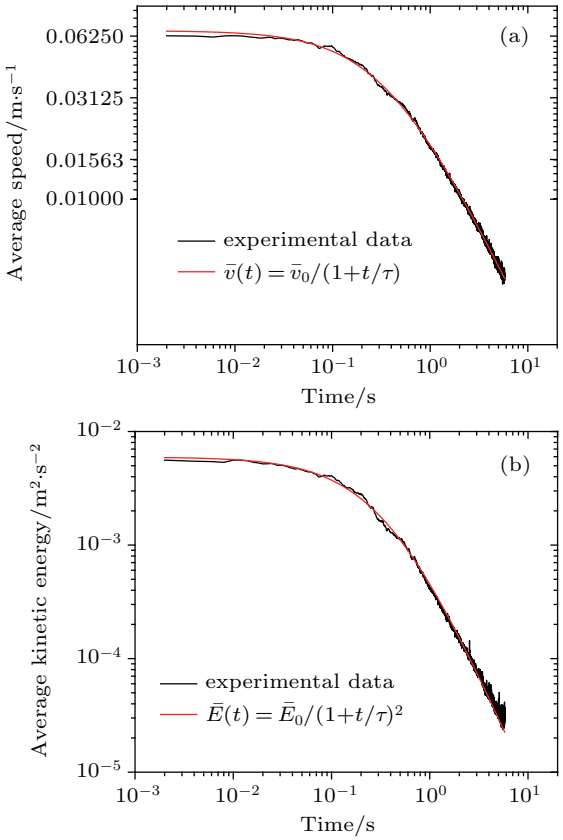


Fig. 4. (color online) (a) Average speed and (b) average kinetic energy of particles as a function of time.

Table 2. Parameters fitted by Eq. (3).

Index	$\bar{v}_0$/(m/s)	τ/s	$\bar{v}_0 \times \tau$/m
1	0.030	0.85	0.026
2	0.066	0.38	0.025
3	0.025	1.08	0.027
4	0.036	0.77	0.028

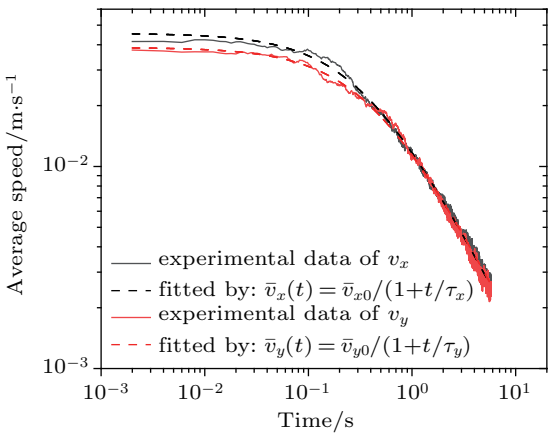


Fig. 5. (color online) Average speeds in the vertical (x, black curves) direction and horizontal (y, red curves) direction decaying with time.

In our experiments, collisions with the two pistons provide particles with initial velocities in the x direction. Figure 5 shows time evolutions of both $\bar{v}_x$ and $\bar{v}_y$, which are consistent with those from Haff's law. Since particles gain velocities in the y direction through particle–particle collisions, the initial $\bar{v}_y$ is seen to be smaller than that of $\bar{v}_x$ due to the dissipation caused by the inelastic collisions. However, we see in Fig. 5 that although initially $\bar{v}_x$ is greater than $\bar{v}_y$, it takes about the same time (approximately 0.5 second) for them to reduce to the same velocity. This again is predicted by Haff's Law. As we can see, when the time t is large enough compared with the characteristic decay time τ, equation (3) becomes

$$\bar{v}(t) \cong \frac{\bar{v}_0}{t/\tau}. \tag{7}$$

Substituting Eq. (4) into Eq. (7), we have

$$\bar{v}(t) = \frac{4}{(1-e^2)n\sigma t}. \tag{8}$$

Equation (8) shows that when $t \gg \tau$, the average speeds do not depend on the initial velocities, and the velocities of different directions converge into the same value. The average velocity depends on the restitution coefficient and the particle number density.

The kinetic energy E is proportional to the square of the average speed of particles $\bar{v}^2$. The kinetic energy of each dimension in the freely cooling state obeys the energy equipartition theorem.

5. Simulation results

Considering the limitation of the experimental opportunities, we perform simulations based on the discrete elements method (DEM).[45,46] The cell size in the simulation is fixed at 10 cm×10 cm×10 cm. In Haff's theory, the contribution of the energy dissipation caused by friction during collision between particles is not considered; however, in reality, friction exists. In this simulation, the influence of friction is considered.

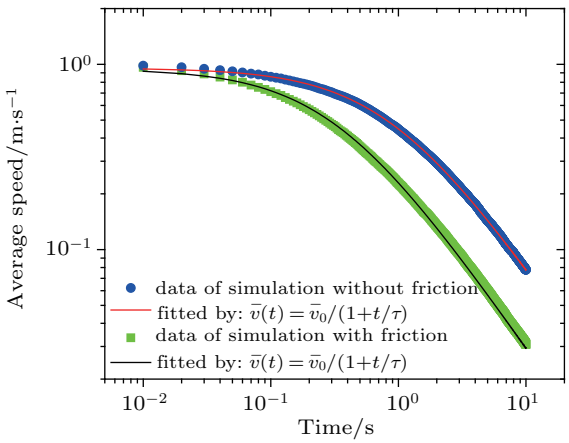


Fig. 6. (color online) Average speeds decaying with time t with (blue dot) and without (green dot) condisering friction.

Figure 6 shows the decays of the simulated average speed with and without considering friction. It is seen that it decays faster when friction is considered. Both can be fitted to Haff's law, but with different values of τ. Haff's freely cooling law is rather robust even though several assumptions in the theory are not satisfied. In the following section, the influence of friction on τ will be discussed.

5.1. Effects of restitution coefficient and friction on characteristic time τ

Figure 7 shows the simulation results for the τ versus restitution coefficient e when friction is not taken into account. The green line is plotted by using Eq. (4). The inset in Fig. 7 shows the linear relationship between τ and $(1-e^2)^{-1}$. When the restitution coefficient e is close to 1, the τ approaches to infinity.

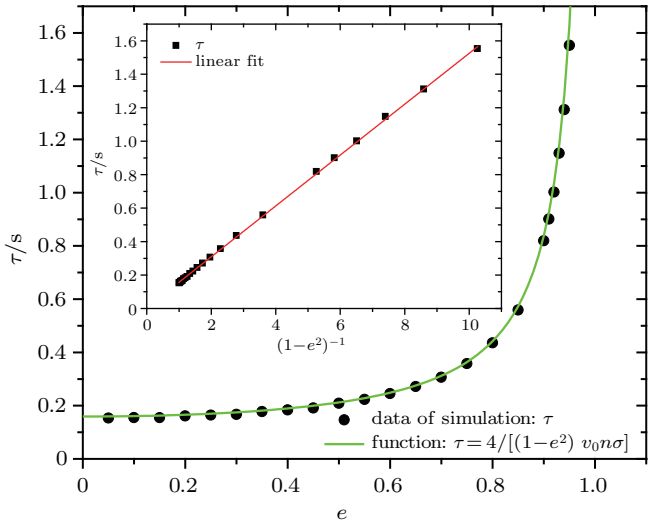


Fig. 7. (color online) Simulated τ versus the restitution coefficient e with no friction. Inset shows the linear relationship between $(1-e^2)^{-1}$.

Figure 8 shows the simulated τ versus restitution coefficient e with taking rotation and friction into account. The inset of Fig. 8 still shows the good linear dependence of τ on $(1-e^2)^{-1}$, however, the intersection shifts. We consider the shift to be due to rotation and friction by adding a γ term $(1-e^2+\gamma)^{-1}$. The total kinetic energy loss after each collision on average is $\Delta E = (1-e^2+\gamma)E$. Equation (4) is thus modified into

$$\tau = \frac{4}{(1-e^2+\gamma)\,\bar{v}_0 n\sigma}. \tag{9}$$

The red curve in Fig. 8 is fitted by Eq. (9), and the inset figure shows a good linear relationship between τ and $(1-e^2+\gamma)^{-1}$. The friction coefficient in this group of simulations is taken to be 0.3, and the corrective frictional term γ fitted by Eq. (9) equals 0.37. Figure 9 shows that the $(1-e^2) \sim 1/\tau$ straight lines with friction and without friction are almost parallel. The difference between the intercepts with x axis of the two lines is 0.38, which is very close to the fitted value 0.37. The above result indicates that our assumption and modification are reasonably good when the influence of friction during the collision among particles is considered.

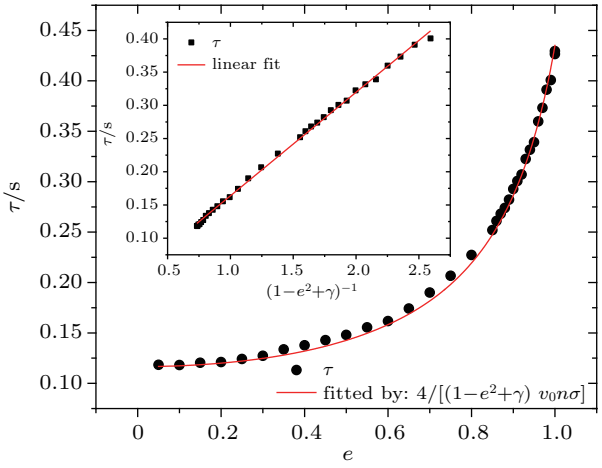


Fig. 8. (color online) Simulated τ versus restitution coefficient e with friction. Inset shows linear relationship between $(1-e^2+\gamma)^{-1}$ and τ.

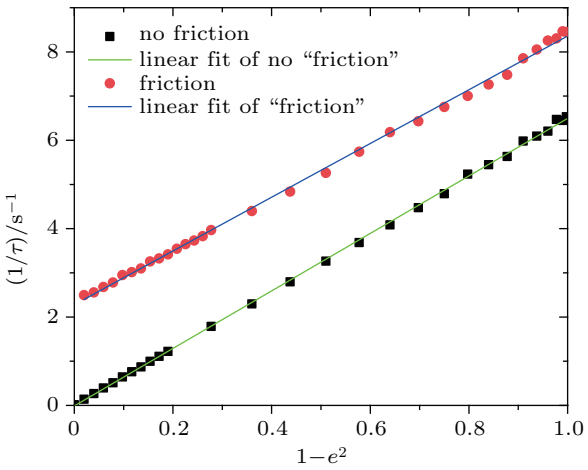


Fig. 9. (color online) Plots of $(1-e^2) \sim 1/\tau$ are both straight lines with and without considering friction. The straight line (blue) with considering friction shifts upward with respect to the straight line (green) without considering friction.

5.2. Effects of number density and particle size on characteristic decay time τ

From Eq. (4) we can see that $1/n$ and $1/R^2$ have a linear relationship with τ respectively. The inset in Fig. 10 shows that the effect of the number density on τ obeys Haff's law while other parameters hold constant, $e = 0.8$, $R = 1$ mm. The inset in Fig. 11 shows that the effect of the size of particles on τ nearly follows Eq. (4), but not strictly, while other parameters hold constant, $e = 0.8$ and $n = 2$ cm^{-3}. We notice that the slope of the curve in the inset gradually becomes upward. This means that the τ will be shorter with a larger size of particles. We recall that an assumption in Haff's law is that the size of particles must be relatively small compared with the mean free path λ of the granular gas system. Actually,

when the size of particles is relatively large compared with λ, we must take into account the size of particles. The collision frequency is accurately related to the average separation s between neighboring particles, which depends on a surface-to-surface distance. A corrective term r_c must be subtracted from the mean free path λ to obtain an average separation s, namely $s = \lambda - r_c$. The corrective term is close to $1.654R$ according to Opsomer's work.[47] The collision frequency Z is calculated from $Z = \bar{u}/s = \bar{u}/(\lambda - 1.654R)$, where $\bar{u}$ is the average relative velocity during collisions among particles. The corrective term will contribute more to the collision frequency when the size of particles turns larger. Hence, the curve $1/\tau \sim R^2$ is a little concave as shown in the inset of Fig. 11.

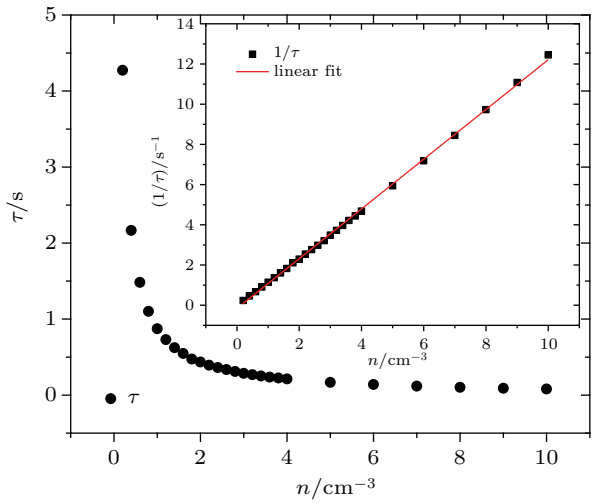


Fig. 10. (color online) Decay time τ as a function of number density n. The inset shows the linear relationship between n and $1/\tau$.

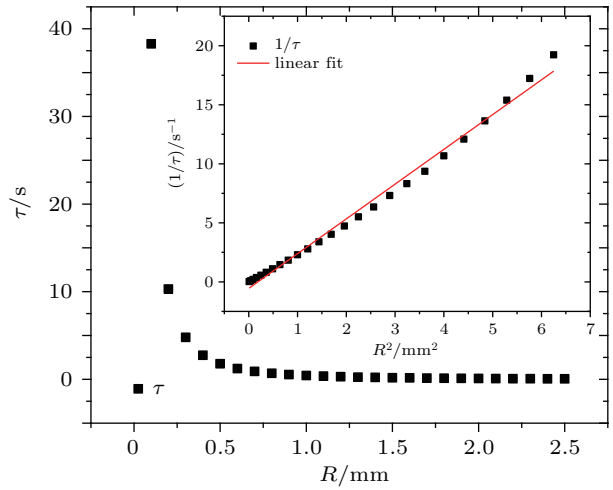


Fig. 11. (color online) Decay time τ as a function of particle radius R. The inset shows $R^2 \sim 1/\tau$ curve slopes upward gradually with respect to linear fitted line.

5.3. Evolution of velocity distribution with time

For a conservative classical ideal gas system in equilibrium state, the velocity distribution of each dimension follows the normal distribution. But it is still not widely accepted that what law the velocity distribution of a dissipative system like granular gas obeys. Figure 12(a) shows that our numerical simulation results of the velocity distribution at different times during the free cooling obey their corresponding normal distribution. The scalar speed of each particle is set to be 1 m/s at the initial time, but the direction of velocity is randomly set. Although the velocity distribution does not satisfy the normal distribution at the initial time, it evolves into the normal distribution after a while. The standard deviation w represents the width of the normal distribution curve. The width is related to the fluctuation of the average speed of particles and is defined as granular temperature. It is verified in Fig. 12(b) that standard deviation w evolving with time t obeys $w \sim (1 + t/\tau)^{-1}$ similar to the average speed of particles.

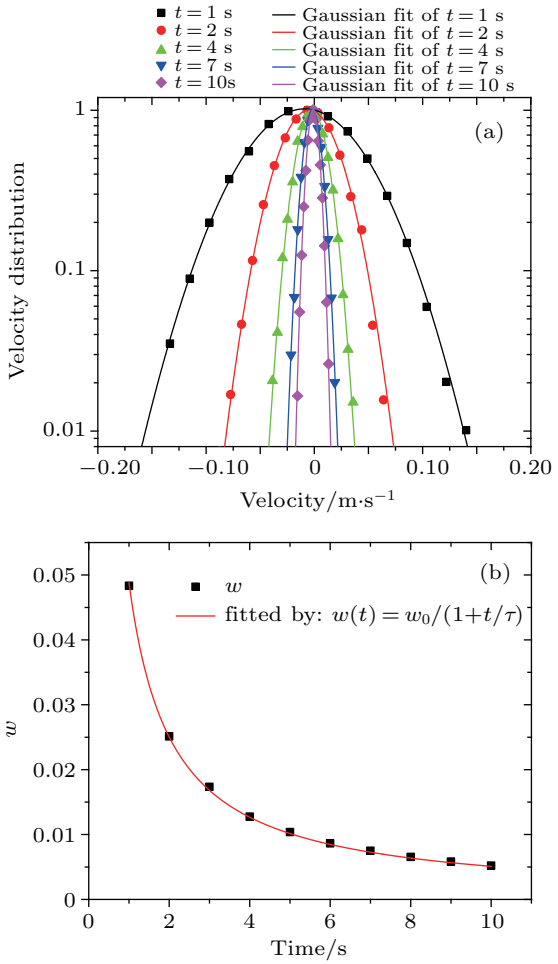


Fig. 12. (color online) (a) Evolutions of velocity distribution in one dimension with time. The number of particles is 10^4. The velocity distribution is standardized. (b) Standard deviation w of the normal distribution varying with time.

We recall that the state of energy equipartitions for freely cooling granular gas will be reached even if the symmetry is broken at the initial time. Our numerical results show that the freely cooling granular gas not only follows Haff's law but also has two intrinsic properties, namely the energy equipartition and the normal velocity distribution.

6. Conclusions

Our experimental and simulation results on the granular gas free cooling process support Haff's law that the kinetic energy dissipates with time t as $E(t) \sim (1+t/\tau)^{-2}$. The effects of particle number density and the particle size on τ, due to the rotation and friction during collision, are studied in simulation. A modified τ is given to take into account the dissipation due to frictions. The collision frequency affected by the number density and particle size is discussed. From the standard deviation of the velocity distribution we also verify the energy dissipation law, showing its good consistence with Haff's Kinetic energy dissipation.

Acknowledgment

We would like to thank Nicolas Vandewalle and Eric Opsomer for their helpful discussion determining the preliminary experimental parameters.

References

[1] Jaeger H M, Nagel S R and Behringer R P 1996 *Rev. Mod. Phys.* **68** 1259
[2] de Gennes P G 1999 *Rev. Mod. Phys.* **71** S374
[3] Kadanoff L P 1999 *Rev. Mod. Phys.* **71** 435
[4] Goldhirsch I I and Zanetti G 1993 *Phys. Rev. Lett.* **70** 1619
[5] McNamara S and Young W R 1994 *Phys. Rev. E* **50** R28
[6] Falcon É Wunenburger R, Évesque P, Fauve S, Chabot C, Garrabos Y and Beysens D 1999 *Phys. Rev. Lett.* **83** 440
[7] Luding S and Herrmann H J 1999 *Chaos* **9** 673
[8] Painter B, Dutt M and Behringer R P 2003 *Physica D* **175** 43
[9] Miller S and Luding S 2004 *Phys. Rev. E* **69** 031305
[10] Efrati E, Livne E and Meerson B 2005 *Phys. Rev. Lett.* **94** 088001
[11] Meerson B and Puglisi A 2005 *Europhys. Lett.* **70** 478
[12] Aranson I S and Tsimring L S 2006 *Rev. Mod. Phys.* **78** 641
[13] Fingerle A and Herminghaus S 2006 *Phys. Rev. Lett.* **97** 078001
[14] Yu P, Frank-Richter S, Börngen A and Sperl M 2014 *Granul. Matter* **16** 165
[15] Chen Y, Pierre E and Hou M 2012 *Chin. Phys. Lett.* **29** 074501
[16] Mei Y, Chen Y, Wang W and Hou M 2016 *Chin. Phys. B* **25** 084501
[17] Wang Y 2017 *Chin. Phys. B* **26** 014503
[18] Haff P K 1983 *J. Fluid Mech.* **134** 401
[19] Brito R and Ernst M H 1998 *Europhys. Lett.* **43** 497
[20] Luding S, Huthmann M, McNamara S and Zippelius A 1998 *Phys. Rev. E* **58** 3416
[21] Garzó V and Dufty J 1999 *Phys. Rev. E* **60** 5706
[22] Huthmann M, Orza J A and Brito R 2000 *Granul. Matter* **2** 189
[23] Zaburdaev V Y, Brinkmann M and Herminghaus S 2006 *Phys. Rev. Lett.* **97** 018001
[24] Hayakawa H and Otsuki M 2007 *Phys. Rev. E* **76** 051304
[25] Meerson B, Fouxon I and Vilenkin A 2008 *Phys. Rev. E* **77** 021307
[26] Santos A and Montanero J M 2009 *Granul. Matter* **11** 157
[27] Kolvin I, Livne E and Meerson B 2010 *Phys. Rev. E* **82** 021302
[28] Mitrano P P, Garzo V, Hilger A M, Ewasko C J and Hrenya C M 2012 *Phys. Rev. E* **85** 041303
[29] Brilliantov N V and Pöschel T 2000 *Phys. Rev. E* **61** 5573
[30] McNamara S and Luding S 1998 *Phys. Rev. E* **58** 2247
[31] Ben-Naim E, Chen S Y, Doolen G D and Redner S 1999 *Phys. Rev. Lett.* **83** 4069
[32] Nie X, Ben-Naim E and Chen S 2002 *Phys. Rev. Lett.* **89** 204301
[33] van Zon J S and MacKintosh F C 2004 *Phys. Rev. Lett.* **93** 038001
[34] Shinde M, Das D and Rajesh R 2007 *Phys. Rev. Lett.* **99** 234505
[35] Shinde M, Das D and Rajesh R 2009 *Phys. Rev. E* **79** 021303
[36] Shinde M, Das D and Rajesh R 2011 *Phys. Rev. E* **84** 031310
[37] Villemot F and Talbot J 2012 *Granul. Matter* **14** 91
[38] Pathak S N, Das D and Rajesh R 2014 *Europhys. Lett.* **107** 44001
[39] Pathak S N, Jabeen Z, Das D and Rajesh R 2014 *Phys. Rev. Lett.* **112** 038001
[40] Maaß C C, Isert N, Maret G and Aegerter C M 2008 *Phys. Rev. Lett.* **100** 248001
[41] Tatsumi S, Murayama Y, Hayakawa H and Sano M 2009 *J. Fluid Mech.* **641** 521
[42] Burton J C, Lu P Y and Nagel S R 2013 *Phys. Rev. Lett.* **111** 188001
[43] Harth K, Trittel T, Wegner S and Stannarius R 2018 *Phys. Rev. Lett.* **120** 214301
[44] Berry M V and Geim A K 1997 *Eur. J. Phys.* **18** 307
[45] Luding S 2008 *Granul. Matter* **10** 235
[46] Wang W, Zhou Z, Zong J and Hou M 2017 *Chin. Phys. B* **26** 044501
[47] Opsomer E, Ludewig F and Vandewalle N 2012 *Europhys. Lett.* **99** 40001